Vol. 25, No. 1(2026) Alim26667

Revista Mexicana de Ingeniería Química

Amylases from malted barley (*Hordeum vulgare*) seeds separated by aqueous two-phase extraction

Amilasas de semillas de cebada (*Hordeum vulgare*) malteada separadas mediante extracción acuosa en dos fases

G. Vega-Ramírez[1], S. Valle-Guadarrama[1]*, B. E. Hernández-Rodríguez[1,2], O. Sandoval-Castilla[1]

[1]Programa de Posgrado en Ciencia y Tecnología Agroalimentaria, Departamento de Ingeniería Agroindustrial. Universidad Autónoma Chapingo, Carretera México-Texcoco km 38.5, Chapingo, 56230, México.

[2]Departamento de Preparatoria Agrícola, Universidad Autónoma Chapingo, Carretera México-Texcoco km 38.5, Chapingo, 56230, México.

Received: September 13, 2025; Accepted: December 16, 2025

Abstract

Germination promotes the production of amylases, making seeds at such stage a source of these enzymes. The objective was to separate amylases from malted barley (*Hordeum vulgare* L.) seeds by aqueous two-phase extraction to facilitate their use in industrial processes. The germination of barley seeds was monitored, showing an increase in protein and enzymatic activity up to maximum values at 42 h, coinciding with a reduction in starch from 63.68 to 48.45%. A mixture of potassium phosphate (PP) and polyethylene glycol 2000 (PEG 2000) was studied to separate amylases by aqueous two-phase extraction. The mixture of 22.03% PP and 17.29% PEG 2000 was chosen, which allowed the enzymes to be recovered in the top polymeric phase, with a yield of 63.92% and a purification factor of 5.82. The enzyme activity was influenced by temperature, pH, and starch concentration, with maximum values of 1.57, 1.81, and 0.98 U mL^{-1} at 40 °C, 5.0, and 0.5%, respectively. The kinetic activity of the amylolytic enzymes was expressed through a Michaelis-Menten model and the effect of inhibition by substrate was discussed. The feasibility of separating amylases from barley germinated seeds through aqueous two-phase extraction was demonstrated.

Keywords: *Hordeum vulgare* L., aqueous two-phase extraction, amylases, barley, germination.

Resumen

La germinación promueve la producción de amilasas, haciendo las semillas en este estado una fuente de estas enzimas. El objetivo fue separar amilasas de semillas malteadas de cebada (*Hordeum vulgare* L.) mediante extracción acuosa en dos fases y así facilitar su uso en procesos industriales. Se monitoreó la germinación de semillas de cebada y se encontró incremento en proteína y actividad enzimática hasta valores máximos a 42 h, coincidiendo con una reducción en almidón de 63.68 a 48.45%. Se usó una mezcla de fosfatos de potasio (FP) y polietilenglicol 2000 (PEG 2000) para separar amilasas mediante extracción acuosa bifásica. Con un sistema que incluyó 22.03% de FP y 17.29% de PEG 2000, se consiguió la recuperación de enzimas en la fase superior con rendimiento de 63.92% y factor de purificación de 5.82. La actividad de las enzimas se afectó por temperatura, pH y concentración de almidón, con valores máximos de 1.57, 1.81 y 0.98 U mL^{-1} a 40 °C, 5.0 y 0.5%, respectivamente. La actividad cinética de las enzimas se expresó por medio de un modelo de Michaelis-Menten y se discutió el efecto de la inhibición por sustrato. Se demostró la factibilidad de separación de amilasas de semillas de cebada germinada mediante extracción acuosa en dos fases.

Palabras clave: *Hordeum vulgare* L., amilasas, cebada, extracción acuosa en dos fases, germinación.

* *Corresponding author. E-mail*: svalleg.chapingo@gmail.com ;

https://doi.org/10.24275/rmiq/Alim26667

ISSN:1665-2738, *issn-e*: 2395-8472

1 Introduction

Malting is an ancient process, dating back thousands of years (Evans *et al*., 2024), which takes advantage of a germination process to transform hard grains such as barley into brittle grains with the starch accessible for beer production (Rani *et al*., 2025). Malting proceeds in three stages, including soaking to ensure water uptake by grains; germination that induces embryo growth, synthesis of enzymes, and partial degradation of the endosperm; and drying, commonly in oven, to stabilize the enzymatic activity of the grain, as well as to induce flavor characteristics and some phytochemical alterations (Polachini et al., 2023; Rani *et al*., 2025; Yang *et al*., 2021). During germination, grains secrete and mobilize hydrolytic enzymes, including amylases and proteases, involved in the breakdown of proteins and starch, to produce amino acids and sugars (Lekjing & Venkatachalam, 2020).

Amylases are hydrolytic enzymes that break down the glycosidic bonds in starch molecules, the main component of cereal seeds (Robles-Arias *et al*., 2025). In addition to their importance in beer brewing (Rani *et al*., 2025), they have applications in other processes, such as detergent production (Gupta *et al*., 2024), the paper industry (Abdel-Nasser *et al*., 2022), the textile industry (Mushtaq *et al*., 2024), the baking industry (Godoy-Ramirez *et al*., 2024; Pismag *et al*., 2023), and wastewater treatment (Gupta *et al*., 2024). Therefore, there is interest in obtaining amylases based on the malting process, for use in various industrial processes, which involves, on the one hand, developing the typical procedure of soaking, germination, and oven drying (Gu *et al*., 2025) and, on the other hand, separating the produced enzymes through an appropriate technique.

Some enzyme purification methods include salting-out precipitation (Abo-Kamer *et al*., 2023), isoelectric point precipitation (Ladjal-Ettoumi *et al*., 2024), ion-exchange chromatography (Phetlum & Champasri, 2023), and ultrafiltration. These methods often need to be combined, as in the case of ammonium sulfate precipitation, where subsequent filtration is required to recover the target enzymes (Shirodkar *et al*., 2020). The costs associated with multi-step purification processes can be high and can represent a considerable proportion of the total production cost (Rao & Haseena, 2024). Therefore, there is a need to explore alternative methods for enzyme purification.

Aqueous two-phase extraction (ATPE) has potential for enzyme separation. Zhu *et al*. (2024) and Singla and Sit (2023) separated papain using systems with aqueous solutions of polyethylene glycol and sodium citrate and polyethylene glycol mixed with ammonium or sodium sulfate, respectively. Likewise, Hasan and Al-Ani (2022) separated peroxidase from corn cobs using a system with aqueous solutions of polyethylene glycol 6000 and ammonium sulfate. In a similar implementation, Šalić *et al*. (2023) used biphasic systems containing ethanol and potassium phosphate to separate lipases.

The aqueous two-phase extraction procedure can, in a single step, separate compounds of interest and address their concentration by non-thermal methods (Rodríguez-Herrera *et al*., 2023). The method uses aqueous mixtures with two immiscible polymers (polyethylene glycol, dextran) or a salt and a polymer (Khan *et al*., 2019) where, depending on the composition, two immiscible phases are formed and, derived from a salting-out phenomenon, the compounds of interest are distributed between the two phases, thus achieving separation (Gomes *et al*., 2017).

The present work focused on the separation of amylases from barley grains using their production from a malting process as a basis. With a similar objective, Girón-Orozco *et al*. (2023) demonstrated the separation from germinating triticale seeds, but they also found that, depending on conditions such as pH, the enzymes can be obtained from one phase or another of the system, so it is not possible to generalize, and the procedure must be investigated for each plant material and each system. Based on these elements, the work aimed to separate amylases from malted barley grains by aqueous two-phase extraction, to promote their use in industrial processes.

2 Materials and methods

2.1 Plant material

Seeds of barley (*Hordeum vulgare* L.), variety Esperanza, from Calpulalpan, Tlaxcala, Mexico (19°35?13? N 98°34?06?W; 2580 meters above sea level) were used. The seeds were cleaned of impurities such as stones, floral remains, ear fragments, and other grains, packed in polyethylene bags sealed under vacuum, and stored at -10 °C until use.

2.2 Protein and enzymatic activity during germination

A batch of 500 g of barley seeds was disinfected through immersion for 5 min in a solution with 0.5% (v/v) of sodium hypochlorite, at 1:3 (w/v) ratio. Successive rinses with distilled water were applied until reaching a pH of 7.0 to remove hypochlorite residues, which was assisted by a potentiometer (HI8424, Hanna Instruments, Inc., Woonsocket, USA). A malting procedure was applied and began

with immersion of seeds in distilled water at 25 ± 1 °C in a polyethylene tray, at 1:3 (w/v, seed/water) ratio, for 36 h, with liquid changes every 12 h, until the plant material reached 42% moisture content, determined with a thermobalance (Ohaus, New Jersey, USA). Excess of water was drained, and the seeds were distributed in polyethylene trays, forming a 2 cm deep layer and incubated at 25 ± 1 °C for germination. Samples of 30 g were taken every 6 h for 84 h, which were dried by lyophilization (Labconco Corp., Model 7755040, USA). A portion of the sample was subjected to starch content determination with the procedure described by Bahdanovich *et al*. (2022), supported by a soluble starch standard curve of 1-10 mg mL^{-1} and with results reported as percentages. The remaining portion was ground during 30 s in a food processor (NutriBullet, CA., USA), with a 20 mM buffer of sodium phosphate (1:5, w/v) pH 6.9, and 6.7 mM sodium chloride, tempered at 4 ºC. The mixture was centrifuged (Ohaus, New Jersey, USA) at 4 °C and 18,947xg during 15 min. The supernatant was again centrifuged under the same conditions for 5 min, and was recovered to be identified as extract, which was subjected to determination of protein content and amylase enzyme activity, through the procedures described in the "*Evaluation of variables*" section. The entire procedure was performed in triplicate.

2.3 Binodal diagram

To prepare an aqueous two-phase extraction process, a binodal diagram was developed. A 40% (w/v) aqueous solution of polyethylene glycol 2000 (PEG 2000) was prepared and also a 40% (w/v) solution that contained 72% dibasic potassium phosphate (K_2HPO_4) and 28% monobasic potassium phosphate (KH_2PO_4). Deionized water was used as solvent. To identify the concentrations corresponding to the binodal curve, the two-stage cloud point procedure described by Rodríguez-Salazar and Valle-Guadarrama (2020) was followed. Batches of five grams of the PEG 2000 solution were weighed in 70 mL Pyrex® tubes, and the phosphate mixture was added dropwise until a cloudy appearance was observed. Subsequently, water was added drop by drop until clarity was obtained, the phosphate mixture addition was repeated until turbidity, and so on. The mixture was weighed at each stage of turbidity or clarity with analytical balance (Ohaus, New Jersey, USA). The procedure was repeated, starting with 5 g of the phosphate mixture, followed by alternating PEG 2000 and deionized water, until turbidity or clarity were observed, respectively.

Mass balance routines (Rodríguez-Salazar & Valle-Guadarrama, 2020) were applied to determine the concentrations of PEG 2000 and potassium phosphate at each turbidity or transparency state with Equations (1) and (2), where $x_{F,\,i}$ and $y_{P,\,i}$ were concentrations (%) of potassium phosphate and PEG 2000 in an ith-mixture, $x_{F,\,i-1}$ and $y_{P,\,i-1}$ were concentrations (%) of potassium phosphate and PEG 2000 in an anterior mixture (i-1), while $x_{F,\,0}$ and $y_{P,\,0}$ were concentrations (%) of the components in the original solutions. Likewise, w_F, w_P, and w_H were masses of mixture of phosphates, PEG 2000, and water added in the ith-stage. Finally, m_{i-1} was the mass of a previous (i-1) mixture. The entire procedure was performed in triplicate.

$$x_{F,i}\,(\%) = \frac{\left(\frac{x_{F,i-1}}{100}\right)(m_{i-1}) + \left(\frac{x_{F,0}}{100}\right)(w_F)}{m_{i-1} + w_F + w_P + w_H} * 100 \qquad (1)$$

$$y_{P,i}\,(\%) = \frac{\left(\frac{y_{P,i-1}}{100}\right)(m_{i-1}) + \left(\frac{y_{P,0}}{100}\right)(w_P)}{m_{i-1} + w_F + w_P + w_H} * 100 \qquad (2)$$

The values of $x_{F,i}$ and $y_{P,i}$ were graphed and formed a binodal curve that separated monophasic conditions and biphasic conditions. In addition, a tie-line was drawn with the method described by Hernández-Rodríguez *et al*. (2025). Briefly, binodal data of $x_{F,\,i}$ and $y_{P,\,i}$ were handled with non-linear regression using the Sigma Plot software (SPSS, 2000) and fitted to Equation (3) (Merchuk *et al*., 1998), where x_{bin} and y_{bin} were binodal concentrations (%) of potassium phosphate and PEG 2000, respectively, while k_1, (%), k_2, ($\%^{-0.5}$) and k_3 ($\%^{-3}$) were regression parameters.

$$y_{bin} = k_1\, exp\left(k_2\, (x_{bin})^{0.5} - k_3\, (x_{bin})^3\right) \qquad (3)$$

The experimental binodal states with the lowest ($x_F^{\min}$) and highest ($x_F^{\max}$) average potassium phosphate concentrations were identified. Thereafter, Equation (3) was used to determine the corresponding concentrations with the highest ($y_P^{\max}$) and lowest ($y_P^{\min}$) PEG 2000 values. Subsequently, states A ($x_F^{\min}$, $y_P^{\max}$; % w/w) and B ($x_F^{\max}$, $y_P^{\min}$; % w/w) were used to draw an experimental tie line, on which four states were identified and labeled as C, D, E, and F, respectively. The systems were prepared with the corresponding concentrations of PEG 2000 and potassium phosphate and were left to stand for 24 h. Biphasic systems were formed, with top (*t*) and bottom (*b*) phases, which were separated, and their volumes (V_t and V_b, respectively) were determined with a graduated cylinder. Thus, the volume ratio (V_r, dimensionless) was calculated with Equation (4) for each state.

$$V_r = \frac{V_t}{V_b} \qquad (4)$$

The method described by Carranza-Gomez *et al*. (2025) was applied to find a state with equal volume partitioning (V_r = 1). To do this, data of volume of top phases (V_t) and the concentration of PEG 2000 (y_P) of states C, D, E, and F, were handled with linear regression and Equation (5) was fitted.

Additionally, data of volume of bottom phases (V_b) and the concentration of potassium phosphate (x_F) of the same states were fitted to Equation (6), where k_4, k_5, k_6, and k_7, were regression constants.

$$V_t = k_4 + k_5\, y_P \tag{5}$$

$$V_b = k_6 + k_7\, x_F \tag{6}$$

Equations (5) and (6) were equated and generated Equation (7). In addition, the concentrations of x_F and y_P were subjected to linear regression and Equation (8) was obtained, where k_8 and k_9 were regression constants. Equations (7) and (8) were simultaneously solved and the condition where volumes of the top and the bottom phases were equal was determined, which was denoted as Z ($x_F^{V_r=1}$, $y_P^{V_r=1}$).

$$y_P = \left(\frac{k_6 - k_4}{k_5}\right) + \left(\frac{k_7}{k_5}\right) x_F \tag{7}$$

$$y_P = k_8 + k_9\, x_F \tag{8}$$

2.4 *Separation of amylases with ATPE*

Aqueous biphasic systems were prepared with the concentrations of potassium phosphate and PEG 2000 corresponding to state Z. Samples of 0.1 g of germinated and freeze-dried (42 h) barley were added in 10-g batches. Mixtures were vortexed (Cole-Parmer, Illinois, USA), allowed to stand for 30 min at 25 ± 1 °C, and centrifuged (Ohaus, New Jersey, USA) for 15 min at 18,947 xg to aid phase formation (Carranza-Gomez *et al*., 2025). The phases of systems were separated, the volume of each phase was measured, and the volume ratio was determined with Equation (4). The separated phases were placed in vials, lyophilized (Labconco Corp., Model 7755040, USA), and subjected to evaluation of protein content and amylase enzyme activity, with the methodologies described in the "*Evaluation of variables*" section. The protein partition coefficient (k_P; Equation 9) and enzymatic activity partition (k_e; Equation 10) were determined, as well as the separation yield (R, %; Equation 11) and the purification factor (F_p; Equation 12) (Panajotova *et al*., 2017), where $c_{p,t}$ and $c_{p,b}$ were concentrations of protein in top (t) and bottom (b) phases, A_t and A_b were enzymatic activity in them, respectively, while AE_t and E_T were the specific activities in the top phase and the total enzyme, respectively.

$$k_P = \frac{c_{p,\,t}}{c_{p,\,b}} \tag{9}$$

$$k_e = \frac{A_t}{A_b} \tag{10}$$

$$R = \frac{100}{(V_r\, k_e)^{-1} + 1} \tag{11}$$

$$F_p = \frac{AE_t}{E_T} \tag{12}$$

2.5 *Effect of temperature, pH and substrate concentration*

The effects of temperature (30-80 °C, pH 6.9, 1% soluble starch), pH (3-8, 37 °C, 1% soluble starch), and starch concentration (0.3-1.5% (m/v), pH 6.9, 37 °C) on the activity of the ATPE-separated amylase enzymes were evaluated using Z-state conditions on the tie line. These evaluations were simultaneously conducted.

2.6 *Kinetic behavior of enzymes*

The relationship between the enzymatic activity and the starch concentration was characterized through a kinetics model (Nelson & Cox, 2009; Verlaine *et al*., 2024). The initial rate of starch degradation (V_0) by the action of amylolitic enzymes was evaluated using starch at concentrations ([S]) of 0.3 (16.65 mM), 0.4 (22.20), 0.5 (27.75), 0.75 (41.63), 1.0 (55.51), and 1.5% (83.26 mM). The mixture was incubated at the optimal temperature and pH conditions during 4 min, and the enzymatic activity (A) or the initial starch consumption rate (V_0; μmol min^{-1} mL^{-1} or U mL^{-1}) was indirectly evaluated through the production of D-glucose with the Equation (13), where c_g, c_g^f, and c_g^0 were D-glucose concentration (mM) at the end (f) and the start (0; assumed equal to zero), and Δt was the reaction time (4 min).

$$A \text{ or } V_0 = -\frac{d[S]}{dt} \cong +\frac{d\left[c_g\right]}{dt} \cong \frac{c_g^f - c_g^0}{\Delta t} \tag{13}$$

It was hypothesized that the starch consumption rate can be affected by the increment of starch concentration. Thus, a substrate inhibition type model was used with the form of Equation (14) (Verlaine *et al*., 2024), where $V_{\max}$ was maximum reaction rate (μmol min^{-1} mL^{-1} or U mL^{-1}), K_M was the Michaelis constant (mM), and K_i (mM) was the inhibition by substrate constant. The starch concentration was again indirectly evaluated through D-glucose concentration.

$$V_0 = \frac{V_{\max}\,[S]}{[S] + K_M + \frac{[S]^2}{K_i}} \tag{14}$$

Based on results of the evaluation of temperature and pH effects, the value of $V_{\max}$ was estimated. Thereafter, K_M and K_i were evaluated with the nonlinear least squares algorithm (*lsqnonlin.m* function) of Matlab® Optimization Toolbox (The Mathworks Inc., 2008), which was applied with the following syntax, where lb established that the search parameters could not be negative, and the empty brackets indicated that there was no upper limit for p(1) and p(2). In addition, the procedure was developed with a maximum of 2000 iterations and a minimum tolerance of 1×10^{-5} in the function.

```
S = [data of starch concentration]';
Vexp = [data of Vo]'; % p(1) = Km,
p(2) = Ki
model = @(p,S) Vmax .* S ./ (p(1) + S
+ (S.^2 ./ p(2)));
fun = @(p) model(p,S) - Vexp;
p0 = [Kmo  Kio]; lb = [0, 0]; ub = [];
opts = optimoptions('lsqnonlin','Display',
'iter');
[p_opt] = lsqnonlin(fun, p0, lb, ub, opts);
Km_opt = p_opt(1); Ki_opt = p_opt(2);
```

2.7 *Evaluation of variables*

The protein content was determined in extracts obtained at different germination times and in the different systems evaluated on the tie line. One hundred microliters of sample reacted with 1900 μL of Bradford (1976) reagent. The mixture was vortexed (Cole-Parmer, Illinois, USA) for 10 s and subsequently the absorbance was measured at 595 nm with spectrophotometer (DR 500 UV-vis HACH, USA). Results were expressed as protein concentration through a standard curve of bovine serum albumin prepared in the range of 0.1 to 1 mg mL^{-1}.

The enzyme activity was evaluated in the extracts obtained at different times of germination and in the states evaluated on the tie line. The procedure described by Miller *et al*. (1960) was implemented with modifications. A mixture with 300 μL of sodium phosphate buffer (20 mM, pH 6.9, and 6.7 mM NaCl), 300 μL of sample, and 150 μL of 1% (w/v) soluble starch was incubated during 10 min at 37 °C. To interrupt the reaction, 3,5 dinitrosalicylic acid (DNS) was added in quantity of 750 μL and boiling was applied in a bath for 5 min. The mixture was cooled, and the absorbance was measured at 540 nm with spectrophotometer (DR 500 UV-vis HACH, USA). Data were analyzed with the aid of a D-glucose standard curve (0.1-1 mg mL^{-1}) and the Equation (13), where Δt was equal to 10 min and the enzymatic activity (A) was expressed in units per mL (U mL^{-1}), defining one unit of amylase activity as the amount of enzyme that produced one micromole of D-glucose per min under the evaluated conditions.

2.8 *Molecular weight estimation*

SDS-PAGE electrophoresis was performed as indicated by Laemmli (1970) to evaluate the molecular weight of the amylases enzymes. The sample obtained at 42 h of germination and top and bottom phases of ATPE systems performed with the Z concentrations state were analyzed. The system consisted of biphasic gels. The stacking phase was a 3% polyacrylamide gel, while the resolving phase was a 12% polyacrylamide gel. Two hundred microliters of each sample were mixed with 600 μL of rupture solution (0.062 M Tris-HCl, 2% SDS, 10% glycerol, 5% 2-mercaptoethanol, and 0.05% bromophenol blue). Boiling was applied for 5 min and 20 μL of the mixture was injected into each lane of the gel. The procedure was performed in a vertical electrophoresis chamber (Thermo Fisher Scientific, Waltham, USA) at constant voltage of 90 V for the stacking gel and 110 V for the resolving gel for 1 h. The gel was removed from the electrophoresis chamber and stained for 1 h with a solution composed of Coomasie blue G-250 (0.1%, w/v), methanol (40%, v/v), acetic acid (10%, v/v), and deionized water (49.9% v/v). Thereafter, destaining for 1 h with a solution composed of methanol (40% v/v), acetic acid (10% v/v), and deionized water (50% v/v) was performed. A molecular weight standard (Thermo Fisher Scientific, Catalog No. 26616, Waltham, USA) of 10 to 170 kDa was taken as reference.

2.9 *Data analysis*

The experimental organization was conducted with completely randomized designs, with germination time, states on binodal phase diagram, and conditions of temperature, pH, and substrate concentration, as variation factors, respectively. Analyses of variance were performed with data of each experiment, together with treatment means comparison routines, using the Tukey test, with a significance level of 0.05. All the tests were performed in triplicate. The goodness of fit of Equations (3), (5), (6), and (8) was evaluated with the determination coefficient (r^2), defined in the form of Equation (15) (Madadi *et al*., 2013), where x_{exp} represents experimental data, x_{mod} data estimated by the model, and x_{mean} the mean value. In this regard, as r^2 was closer to unity the fitting of data to the model was considered adequate.

$$r^2 = 1 - \frac{\sum_1^n \left(x_{\text{exp}} - x_{mod}\right)^2}{\sum_1^n \left(x_{\text{exp}} - x_{mean}\right)^2} \tag{15}$$

3 Results and discussion

3.1 *Starch, protein, and enzymatic activity during germination*

The barley seed presented starch content of 63.68% (±0.17) and during germination the concentration of this polysaccharide decreased rapidly in the first 42 h and then stabilized at an average value of 48.45% (±0.26) (Fig. 1a). The decrement of starch content during germination has been reported for other cereal grains, although Edleman *et al*. (2025) indicated that such phenomenon is a function of temperature. Sofi *et al*. (2023) pointed out that

germination promotes hydrolysis of starch in the endosperm of the seeds. Although the case of β-amylase is scarcely documented, it has been reported that α-amylase, the most common amylolytic enzyme, catalyzes the hydrolysis of α-(1,4) glycosidic bonds in starch polymers, causing its depolymerization (Wang *et al*., 2022).

Furthermore, germination causes swelling and some level of gelatinization in starch granules, which disrupts their ordered structure (Zheng *et al*., 2024). Therefore, starch content decreases during germination (Kaur *et al*., 2024), as does amylase activity. However, only 25% of the total available starch content is utilized (Van de Velde *et al*., 2025) and is subsequently used for seedling development (Li *et al*., 2023).

Protein content increased consistently with germination time, from an initial value of 10.46 mg mL^{-1} to a maximum of 26.73 mg mL^{-1} at 42 h. However, a decrement to 18.20 mg mL^{-1} was observed upon completion of 84 h of process (Figure 1b). The increase in protein content is a phenomenon that accompanies the germination of a seed (Xie *et al*., 2025). In this regard, the increase in protein occurs because the seed synthesizes proteases, lipases, and amylases for the hydrolysis of storage reserves, such as hordeins, hordenines, starch, and lipids, which provide energy to the embryo for the development of a new plant (Alu'datt *et al*., 2019; Jones, 2005; Obadi *et al*., 2021).

Consistently, the activity of the amylase enzyme increased significantly during the first 42 h of germination, from an initial value of 4.17 U mL^{-1}, reaching a maximum value of 11.42 U mL^{-1}, and then decreasing to a value of 4.93 U mL^{-1} at 84 h of process (Figure 1c), which was consistent with the variation in starch content. On this basis, the conditions of 42 h and 25 °C were chosen as adequate to conduct the germination process of barley seeds.

On the other hand, the evaluation of the enzymatic activity used an immersion procedure in a mixture of a sodium phosphate buffer and sodium chloride at 4 °C, followed by homogenization in a domestic blender for 30 s, which was like the procedure applied by Posoongnoen *et al*. (2025). When immersion milling of a solid sample is performed to extract enzymes, the mechanical process and the medium conditions can have both positive and negative effects on the enzymatic proteins. In principle, milling breaks down cell walls, membranes, and the extracellular matrix, increasing the availability of intracellular enzymes and facilitating their solubilization in the buffer. It also increases the surface area, promoting contact between the solid and the extracting solution. Furthermore, the disruption of the compartmentalized structure can favor enzyme separation. However, negative effects can occur, such as frictional heating resulting from

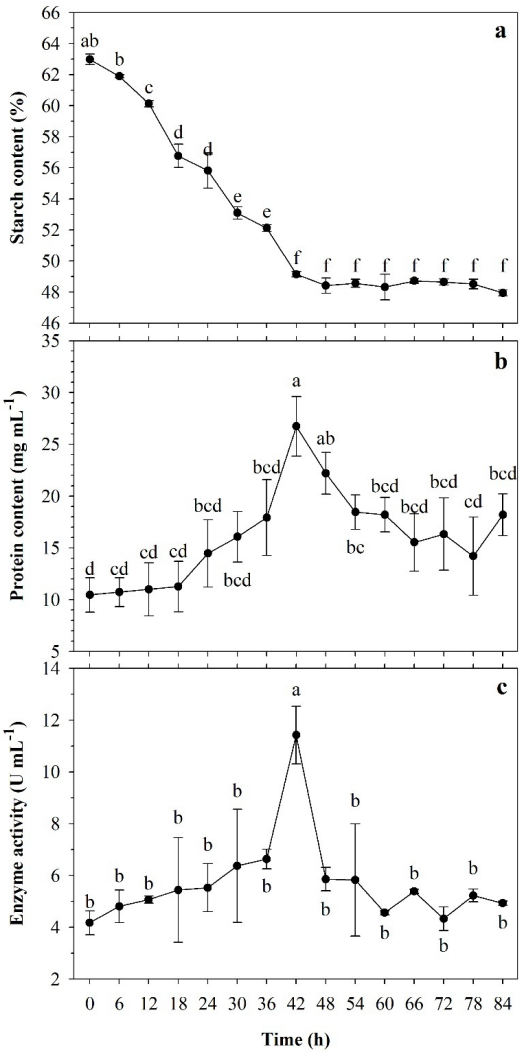

Fig. 1. Starch content (a), protein content (b), and amylase enzyme activity (c) in barley seeds during germination. Equal letters indicate non-significant differences (Tukey, 0.05).

mechanical action. However, if the temperature does not exceed 40 °C, protein denaturation cannot be considered a significant factor. In the work, the mechanical treatment was applied at 4 °C for only 30 s, as the germinated seeds were in a freeze-dried state and milled easily. On the other hand, the mechanical effect caused by the food processor blades can cause mechanical stress, which could induce loss of protein structure. However, the turbulence involved and the resulting heating led to better imbibition of the freeze-dried material.

3.2 Binodal phase diagram

The mixture with polyethylene glycol 2000 and potassium phosphate showed potential to form biphasic systems. The cloud point procedure allowed identifying binodal states that delimited conditions where the mixture formed a homogeneous solution

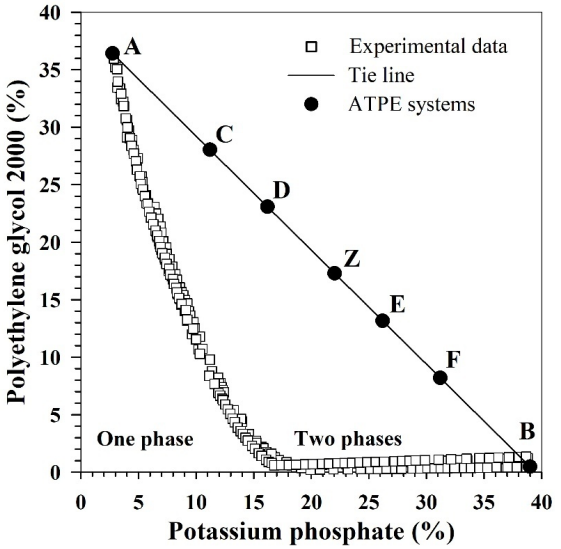

Fig. 2. Binodal phase diagram of the PEG 2000 and potassium phosphate system. A, B, …, F: evaluated biphasic systems.

in a single liquid phase from conditions where a heterogeneous mixture was formed and separated into two immiscible phases (Fig. 2).

The binodal data fitted well (r^2=0.9977±0.0002) to Equation (3), and values of 80.0303 (±4.8307), −0.4698(±0.0314), and 4.3995×10^{-4} (±2.6784×10^{-5}) were obtained for constants k_1, k_2, and k_3, respectively. With this basis, the average experimental conditions with the lowest and highest potassium phosphate concentrations were identified and, with the support of Equation (3), states A (2.7452, 36.4138%) and B (38.9925, 0.4832%) were also recognized. With this information, an experimental tie line was drawn (Figure 2) and states C (11.2000, 28.0329%), D (16.2000, 23.0766%), E (26.2000, 13.1639%), and F (31.2000, 8.2076%) were identified on it (Fig. 2), which were used to prepare systems in physical form. All these systems formed two-phases. The volume of top phases was related to the PEG 2000 concentration of systems C, D, E, and F (Equation 5). Likewise, the volume of bottom phases was related to the potassium phosphate concentrations (Equation 6). By equating models, Equation (7) was obtained with values of 8.8462, -0.2299, 6.4991, and -0.1572 in the constants k_4, k_5, k_6, and k_7, respectively. Likewise, the concentrations of PEG 2000 and potassium phosphate were related, from which the values of 39.4799 and -1.0088 were obtained for the constants k_8 and k_9. With this, Equations (7) and (8) were solved, and the system Z (22.03, 17.29%) was obtained, which corresponded to the two-phase condition with equal volume partitioning (V_r=1).

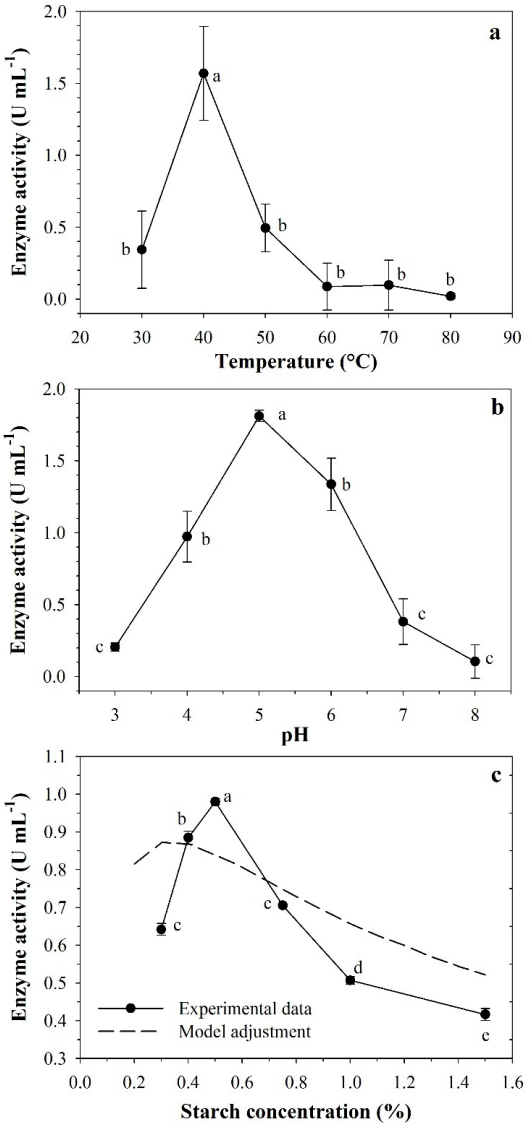

Fig. 3. Effect of temperature (a), pH (b), and substrate concentration (c) on amylase enzyme activity. Equal letters indicate a non-significant difference (Tukey, 0.05).

3.3 Characterization of amylase purification

The system formulated for the state Z in the binodal diagram separated into two phases, a top phase (*t*) and a bottom phase (*b*). This separation caused protein concentrations of 0.17±0.03 mg mL^{-1} in the top phase and 1.47±0.11 mg mL^{-1} in the bottom phase, resulting in protein partition coefficient of 0.12±0.03 (Equation 9), which indicated that proteins migrated primarily to the bottom phase. However, the amylase enzyme activity had a value of 1.35±0.02 U mL^{-1} in the top phase and a value of 0.64±0.01 U mL^{-1} in the bottom phase, indicating that amylases migrated mainly to the top phase, which generated the value of 2.12±0.02 in the partition coefficient of the enzyme activity (Equation 10). In this regard, Kavakçioğlu &

Tarhan (2013), pointed out that a high value of k_e accompanied by a low value of k_p indicates that the enzymatic fraction is concentrated to a greater extent in the top phase, which confirmed that the aqueous two-phase extraction technique has the potential to address the purification of enzymes. In addition, this technique favors the preservation of the bioactivity of the separated molecules, due to the high content of water in both the top and bottom regions, which varies between 80 and 90%, and provides an environment close to the natural conditions where biomolecules are usually found (Shad *et al*., 2018). Furthermore, the gentle nature of the process, which avoids using aggressive organic solvents, permits the protection of sensitive biomolecules, facilitating the purification of proteins without compromising their biological activity.

On the other hand, the system presented an enzyme separation yield (Equation 11) of 63.92% ± 0.47 and a purification factor (Equation 12) of 5.82 ± 0.87. In this regard, conventional protocols used to purify enzymes require long time to achieve considerable yields and purification (Moreira *et al*., 2013). In this sense, Liaqat *et al*. (2024) purified amylases by precipitation of ammonium sulfate, membrane dialysis, and gel filtration chromatography, and found a factor of purification of 4 and a yield of 13%. Likewise, Fincan *et al*. (2021) mentioned a 30% yield in the purification of α-amylase synthesized by *Bacillus licheniformis* when ammonium sulfate precipitation was used, followed by ion exchange chromatography, and finally, dialysis. In addition, in large-scale processes, multi-step purification reduces enzyme activity and yield (Shad *et al*., 2018).

3.4 Effect of temperature, pH, and substrate concentration

The activity of the enzyme separated by aqueous two-phase extraction showed to be sensible to temperature, in a way that, starting from 0.34 (±0.27) U mL^{-1}, it increased to a maximum of 1.57 (±0.33) U mL^{-1} at 40 °C, and then consistently decreased to 0.02 (±0.02) U mL^{-1} at 80 °C (Fig. 3a). The optimal temperatures for alpha and beta amylases are different. According to De Schepper *et al*. (2022), between 40 and 60 °C there is no difference in the residual activity of alpha amylases, while between 40 and 50 °C there is no difference in that of beta amylases. In this regard, the optimal temperature that was found in the present work was within such intervals.

The pH also affected the enzyme activity, since the activity was 0.20 (±0.03) U mL^{-1} at pH 3.0, but increased to a maximum of 1.81 (±0.04) U mL^{-1} at pH 5.0 and then decreased consistently to 0.10 (±0.17) U mL^{-1} at pH 8.0 (Figure 3b). The pH is a variable that can affect the chemical structure of materials (García-Cerqueda *et al*., 2025). In the present work, the behavior can be attributed to changes in the protonation or deprotonation of functional groups of amino acids that are present in the active sites of the enzyme, which causes an alteration in its three-dimensional structure and, consequently, its denaturation (Fincan *et al*., 2021). Likewise, enzymatic denaturation at high pH can prevent adequate interaction with substrates, affecting its ability to catalyze starch hydrolysis efficiently. On the other hand, the present work evaluated a cocktail of enzymes, where different amylases can be present, and each one can exhibit different optimum pH. In this regard, Roth *et al*. (2019) evaluated three microbial α-amylases and determined that all of them had optimum pH around 5.0, which coincided with data of the present work. However, Duan *et al*. (2021) reported that the optimum pH of a microbial β-amylase was 6.5, thus the hypothesis of higher presence of α-amylase can be established.

The enzyme activity was also dependent on the starch concentration present in the medium, since a value of 0.64 (±0.02) U mL^{-1} was obtained with 0.3% substrate, but increased to a maximum of 0.98 (±0.01) U mL^{-1} with 0.5%, and then decreased continuously to 0.42 (±0.02) U mL^{-1} with 1.5% concentration (Fig. 3c). A kinetic behavior consistent with the Michaelis-Menten model corresponds to a situation where the reaction rate or the enzyme activity increases to a maximum, derived from a saturation phenomenon and, from there, the reaction rate becomes constant (Nelson & Cox, 2009). However, the upward trend to a maximum, followed by a continuous decline, suggests a situation of inhibition by substrate, which leads to a drop in reaction rate once the substrate exceeds an optimum concentration. In this regard, an excess of substrate can transiently block access to catalytic sites, and complexes can form between the enzyme and insoluble or highly branched regions of the starch, hindering product release (Segel, 1993). Specifically, as the starch concentration increases, the hydrogen bonds between the substrate and water are partial or completely replaced, which negatively affects the interaction between amylase and its substrate, thus decreasing its catalytic efficiency (Sudeep *et al*., 2020).

In order to verify this situation, the value of 1.81 U mL^{-1} obtained previously was accepted to be $V_{\max}$ in Equation (14). Thus, a nonlinear least squares algorithm (*lsqnonlin.m* function; The Mathworks Inc., 2008) was applied and indicated a value for the Michaelis constant (K_M) equal to 0.1795% (9.96 mM) and an inhibition constant (K_i) equal to 0.6422% (35.64 mM), which indicated that the amylolytic enzymes can tolerate a starch concentration of less than 0.64% before they begin to be inhibited. However, the determination coefficient (r^2) was 0.618,

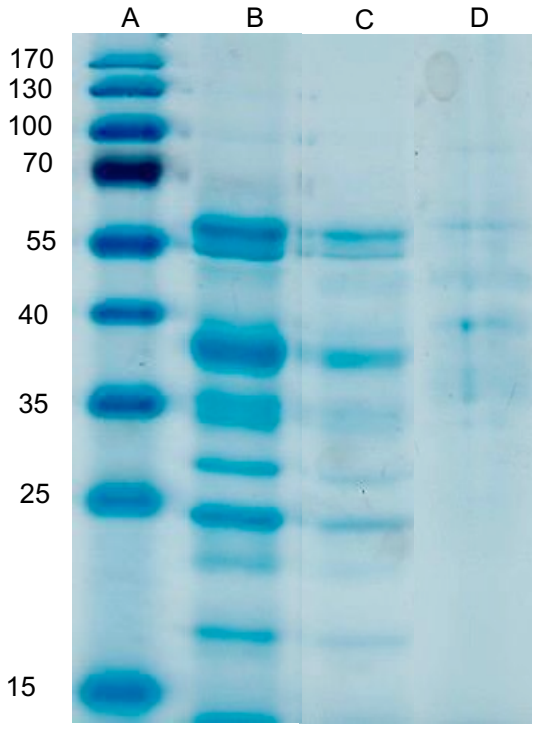

Fig. 4. Analysis of amylases by SDS-polyacrylamide gel electrophoresis. Lane A: standard proteins (kDa). Lane B: germinated barley. Lane C: polymeric phase (top) amylases of the ATPE system. Lane D: salt phase (bottom) amylases of the ATPE system.

which indicated that the data are not entirely consistent with a simple Michaelis-Menten model with substrate inhibition (Fig. 3c), suggesting that the downward trend after the peak was additionally caused by factors other than substrate inhibition. In this regard, an increase in substrate can cause an increase in the viscosity of the medium or can form aggregates or clumps, which impedes the diffusion of the enzyme to the substrate (Segel, 1993).

3.5 Molecular weight of amylases

The electrophoresis analysis of the germinated barley seeds showed the presence of protein bands located at approximately 55, 38, 35, 28, 24, and 18 kDa (Lane B, Fig. 4). Meanwhile, the analysis of the polymeric phase (top phase) of the ATPE systems showed three protein bands of higher concentration, located at approximately 55, 38, and 24 kDa, suggesting the presence of distinct protein structures in this phase. In this regard, given the higher enzymatic activity in this phase, it was hypothesized that there were distinct enzymatic structures in the analyzed phase. In addition, the analysis of the bottom phase of systems showed very faint bands, indicating low concentrations of these structures. The molecular weights of cereal amylases are quite variable, ranging from 45 to 67.2 kDa (BRENDA Enzyme Database, 2025). Previous studies have even reported the activity of germinated barley amylases with molecular weight of approximately 27 kDa. It has also been observed that these enzymes may be associated with the activity of other enzymes, like β-glucanases, which play a complementary role in the polysaccharide hydrolysis process (Herrera-Gamboa *et al*., 2018; Uno-Okamura *et al*., 2004).

Conclusions

The germination of barley seeds caused an increase in the amylases enzymes, with maximum activity at 42 h, which resulted in partial starch degradation. The separation of amylases was feasible from the top phase of a system of aqueous two-phase extraction formed with potassium phosphate and polyethylene glycol. The enzyme activity was affected by variations in temperature and pH. The relationship between the enzyme activity and the starch concentration was partially explained by a Michaelis-Menten model with inhibition by substrate. The feasibility of separating the amylase enzyme produced by germination of barley seeds based on aqueous two-phase extraction was demonstrated. However, data corresponds to a cocktail of enzymes, so it is advisable to conduct the identification and characterization of the specific amylases.

Acknowledgements

Authors are grateful for the support received from the scholarship program of the Secretaría de Ciencias, Humanidades, Tecnología e Innovación (SECIHTI) of Mexico.

Nomenclature

A_t, A_b	Enzymatic activity in the top and bottom phases (U mL^{-1}).
E_T	Total enzyme activity (U mL^{-1}).
F_p	Purification factor (dimensionless).
K_M	Michaelis constant (g L^{-1}).
V_b	Volume of the bottom phase (mL).
$V_{\max}$	Maximum starch consumption rate (g L^{-1} min^{-1}).
V_r	Volume ratio (dimensionless).
V_t	Volume of the top phase (mL).
c_g^0, c_g^f	D-glucose concentration at initial and final determination (mM).
$c_{p,\,t}$, $c_{p,\,b}$	Protein concentrations (mg mL^{-1}) in top (t) and bottom (b) phases.

k_1	Regression constant (%).
k_2	Regression constant ($\%^{-0.5}$).
k_3	Regression constant ($\%^{-3}$).
k_4, k_6, k_8	Regression constants (mL).
k_5, k_7, k_9	Regression constants (mL $\%^{-1}$).
k_P	Protein partition coefficient (dimensionless).
k_e	Partition of enzymatic activity (mg mL^{-1}).
m_{i-1}	Mass of the previous (i-1) mixture.
w_F	Mass (g) of mixture of phosphates added in the ith-stage.
w_H	Mass (g) of water added in the ith-stage.
w_P	Mass (g) of PEG 2000 added in the ith-stage.
$x_{F,\ i}$	Concentration (%) of potassium phosphate in an ith-mixture.
$x_{F,0}$	Concentration (%) of potassium phosphate in the original solution.
$x_{F,i-1}$	Concentration (%) of potassium phosphate in a previous (i-1) mixture.
x_F	Concentration (%) of potassium phosphate in biphasic systems.
$x_F^{\max}$	Maximum experimental binodal concentration (%) of potassium phosphate.
$x_F^{\min}$	Minimum experimental binodal concentration (%) of potassium phosphate.
x_{bin}	Binodal concentration (%) of potassium phosphate.
$y_{P,\ i}$	Concentration (%) of PEG 2000 in an ith-mixture.
$y_{P,0}$	Concentration (%) of PEG 2000 in the original solution.
$y_{P,i-1}$	Concentration (%) of PEG 2000 in a previous (i-1) mixture.
y_P	Concentration of PEG 2000 in biphasic systems.
$y_P^{\max}$	Maximum experimental binodal concentration (%) of PEG 2000.
$y_P^{\min}$	Minimum experimental binodal concentration (%) of PEG 2000.
y_{bin}	Binodal concentration (%) of PEG 2000.
$[S]$	Substrate (starch) concentration (g L^{-1}).
R	Separation yield (%).
V	Starch consumption rate (g L^{-1} min^{-1}).

References

Abdel-Nasser, M., Abdel-Maksoud, G., Abdel-Aziz, M.S., Darwish, S.S., Hamed, A.A. and Youssef, A.M. (2022). Evaluation of the efficiency of nanoparticles for increasing α-amylase enzyme activity for removing starch stain from paper artifacts. *Journal of Cultural Heritage*, *53*, 14–23. https://doi.org/10.1016/j.culher.2021.11.004

Abo-Kamer, A.M., Abd-El-salam, I.S., Mostafa, F.A., Mustafa, A.E.R.A. and Al-Madboly, L.A. (2023). A promising microbial α-amylase production, and purification from Bacillus cereus and its assessment as antibiofilm agent against *Pseudomonas aeruginosa* pathogen. *Microbial Cell Factories*, *22*(1), 141. https://doi.org/10.1186/s12934-023-02139-6

Alu'datt, M.H., Rababah, T., Alhamad, M.N., Gammoh, S., Alkhaldy, H.A., Al-Mahasneh, M.A., Tranchant, C. C., Kubow, S. and Masadeh, N. (2019). Fermented malt beverages and their biomedicinal health potential: Classification, composition, processing, and bio-functional properties. In *Fermented Beverages* (pp. 369–400). Elsevier.

Bahdanovich, P., Axelrod, K., Khlystov, A. Y. and Samburova, V. (2022). Optimized spectrophotometry method for starch quantification. *Analytica*, *3*(4), 394–405. https://doi.org/10.3390/analytica3040027

Bradford, M. M. (1976). A rapid and sensitive method for the quantitation of microgram quantities of protein utilizing the principle of protein-dye binding. *Analytical Biochemistry*, *72*(1–2), 248–254. https://doi.org/10.1016/0003-2697(76)90527-3

BRENDA Enzyme Database. (2025). *N*. https://www.brenda-enzymes.org/index.php Accessed: June 25, 2025.

Carranza-Gomez, M., Valle-Guadarrama, S., Domínguez-Puerto, R., Sandoval-Castilla, O. and Guerra-Ramírez, D. (2025). Bioactive compounds and pigmenting potential of Vaccinium corymbosum extracts separated with aqueous biphasic systems aided by centrifugation. *Processes*, *13*(4), 1072. https://doi.org/10.3390/pr13041072

De Schepper, C.F., Buvé, C., Van Loey, A.M. and Courtin, C.M. (2022). A kinetic study on the thermal inactivation of barley malt α-amylase and β-amylase during the mashing process. *Food Research International*, *157*, 111201. https://doi.org/10.1016/j.foodres.2022.111201

Duan, X., Zhu, Q., Zhang, X., Shen, Z. and Huang, Y. (2021). Expression, biochemical

and structural characterization of high-specific-activity β-amylase from *Bacillus aryabhattai* GEL-09 for application in starch hydrolysis. *Microbial Cell Factories*, *20*(1), 182. https://doi.org/10.1186/s12934-021-01649-5

Edleman, D., Welsh, K., Sweet, L., Murai, T. and Annor, G.A. (2025). Impact of germination time and temperature on starch viscosity properties and chemical composition of intermediate wheatgrass (*Thinopyrum intermedium*). *Journal of Cereal Science*, *122*, 104129. https://doi.org/10.1016/j.jcs.2025.104129

Evans, D.E., Shen, W. and Brookes, P. (2024). Malting - 'the middle parts of fortune' - a history of innovation and the enduring quest for efficiency. *Journal of the Institute of Brewing*, *130*(3), 126–181. https://doi.org/10.58430/jib.v130i3.58

Fincan, S.A., Özdemir, S., Karakaya, A., Enez, B., Mustafov, S.D., Ulutaş, M. S. and Şen, F. (2021). Purification and characterization of thermostable α-amylase produced from *Bacillus licheniformis* So-B3 and its potential in hydrolyzing raw starch. *Life Sciences*, *264*, 118639. https://doi.org/10.1016/j.lfs.2020.118639

García-Cerqueda, C., Rodríguez-Ramírez, J. and Méndez-Lagunas, L. (2025). Kinetic modeling of solid-liquid extraction of mucilage from *Opuntia ficus indica*. *Revista Mexicana de Ingeniería Química*, *24*(1), 1–13. https://doi.org/10.24275/rmiq/Cat24441

Girón-Orozco, D., Mariezcurrena-Berasain, M.D., Aguilar, O., Ramírez-Dávila, J.F. and Heredia-Olea, E. (2023). Recovery of amylolytic enzymes from triticale malt (*X. Triticosecale* Wittmack) using two-phase aqueous systems. *Research Square*, 1–24. https://doi.org/10.21203/rs.3.rs-2468244/v1

Godoy-Ramirez, A., Rodriguez-Huezo, M.E., Lara-Corona, V.H., Vernon-Carter, E.J. and Alvarez-Ramirez, J. (2024). Wheat bread supplemented with potato peel flour: color, molecular organization, texture and in vitro starch digestibility. *Revista Mexicana de Ingeniería Química*, *23*(1), 1–18. https://doi.org/10.24275/rmiq/Alim24201

Gomes, J., Ferreira, S., Reinert, O., Gandol, R., Ayra, L., Santos, V., Veloso, C.M., Ilh, C., Cristina, R. and Bonomo, F. (2017). Evaluation of salting-out effect in the liquid e liquid equilibrium of aqueous two-phase systems composed of 2-propanol and Na2SO4/MgSO4 at different temperatures. *Fluid Phase Equilibria*, *450*, 184–193. https://doi.org/10.1016/j.fluid.2017.08.001

Gu, Z., Rao, J. and Chen, B. (2025). Application of flavoromics approach to evaluate aroma characteristics in malts: Current trends and future outlooks. *Trends in Food Science & Technology*, *156*, 104878. https://doi.org/10.1016/j.tifs.2025.104878

Gupta, N., Paul, J.S. and Jadhav, S.K. (2024). Chitosan decorated magnetic nanobiocatalyst of *Bacillus* derived α-amylase as a role model for starchy wastewater treatment, detergent additive and textile desizer. *Bioorganic Chemistry*, *151*, 107673. https://doi.org/10.1016/j.bioorg.2024.107673

Hasan, H.R. and Al-Ani, A.W. (2022). An economical source for peroxidase: maize cobs. *Karbala International Journal of Modern Science*, *8*(2), 112–122. https://doi.org/10.33640/2405-609X.3227

Hernández-Rodríguez, G., Valle-Guadarrama, S., Guerra-Ramírez, D., Domínguez-Puerto, R. and López-Cruz, I.L. (2025). Anthocyanins of *Ardisia* spp. fruits separated with pH driven-aqueous biphasic systems. *Separation Science and Technology*, *60*(3–5), 426–437. https://doi.org/10.1080/01496395.2024.2445006

Herrera-Gamboa, J.G., López-Alvarado, C.B., Pérez-Ortega, E., Damas-Buenrostro, L.C., Cabada-Amaya, J.C. and Pereyra-Alférez, B. (2018). Proteomic analysis of two malting barleys (*Hordeum vulgare* L.) and their impact on wort quality. *Journal of Cereal Science*, *80*, 150–157. https://doi.org/10.1016/j.jcs.2018.02.004

Jones, B.L. (2005). Endoproteases of barley and malt. *Journal of Cereal Science*, *42*(2), 139–156. https://doi.org/10.1016/j.jcs.2005.03.007

Kaur, N., Gasparre, N. and Rosell, C.M. (2024). Expanding the application of germinated wheat by examining the impact of varying alpha-amylase levels from grain to bread. *Journal of Cereal Science*, *120*, 104059. https://doi.org/10.1016/j.jcs.2024.104059

Kavakçioğlu, B. and Tarhan, L. (2013). Initial purification of catalase from *Phanerochaete chrysosporium* by partitioning in poly(ethylene glycol)/salt aqueous two phase systems. *Separation and Purification Technology*,

105, 8–14. https://doi.org/10.1016/j.seppur.2012.12.011

Khan, B.M., Cheong, K.L. and Liu, Y. (2019). ATPS: "aqueous two-phase system" as the "answer to protein separation" for protein-processing food industry. *Critical Reviews in Food Science and Nutrition*, *59*(19), 3165–3178. https://doi.org/10.1080/10408398.2018.1486283

Ladjal-Ettoumi, Y., Douik, L.H., Hamadi, M., Abdullah, J.A.A., Cherifi, Z., Keddar, M.N., Zidour, M. and Nazir, A. (2024). Physicochemical and functional properties of spirulina and chlorella proteins obtained by iso-electric precipitation. *Food Biophysics*, *19*(2), 439–452. https://doi.org/10.1007/s11483-024-09836-8

Laemmli, U.K. (1970). Cleavage of structural proteins during the assembly of the head of bacteriophage T4. *Nature*, *227*(5259), 680–685. https://doi.org/10.1038/227680a0

Lekjing, S. and Venkatachalam, K. (2020). Effects of germination time and kilning temperature on the malting characteristics, biochemical and structural properties of HomChaiya rice. *RSC Advances*, *10*(28), 16254–16265. https://doi.org/10.1039/D0RA01165G

Li, Q., Zhai, W., Wei, J. and Jia, Y. (2023). Rice lipid transfer protein, OsLTPL23, controls seed germination by regulating starch-sugar conversion and ABA homeostasis. *Frontiers in Genetics*, *14*. https://doi.org/10.3389/fgene.2023.1111318

Liaqat, U.S., Naz, S. and Hussain, H.I. (2024). Optimization and production of highly stable amylase isolated from *Citrobacter portucalensis* using low-cost agro-industrial wastes as substrates: Prospective therapeutics. *Kuwait Journal of Science*, *51*(1), 100156. https://doi.org/10.1016/j.kjs.2023.11.005

Madadi, B., Pazuki, G. and Nasernejad, B. (2013). Partitioning of cefazolin in biocompatible aqueous biphasic systems based on surfactant. *Journal of Chemical & Engineering Data*, *58*(10), 2785–2792. https://doi.org/10.1021/je4004756

Merchuk, J. C., Andrews, B. A. and Asenjo, J. A. (1998). Aqueous two-phase systems for protein separation studies on phase inversion. *Journal of Chromatography B*, *711*, 285–293. https://doi.org/10.1016/S0378-4347(97)00594-X

Miller, G.L., Blum, R., Glennon, W.E. and Burton, A.L. (1960). Measurement of carboxymethylcellulase activity. *Analytical Biochemistry*, *1*(2), 127–132. https://doi.org/10.1016/0003-2697(60)90004-X

Moreira, S., Silvério, S.C., Macedo, E.A., Milagres, A.M.F., Teixeira, J.A. and Mussatto, S.I. (2013). Recovery of *Peniophora cinerea* laccase using aqueous two-phase systems composed by ethylene oxide/propylene oxide copolymer and potassium phosphate salts. *Journal of Chromatography A*, *1321*, 14–20. https://doi.org/10.1016/j.chroma.2013.10.056

Mushtaq, B., Nawab, Y., Ahmad, S. and Ahmad, F. (2024). An eco-friendly enzymatic treatment to prepare spinnable banana fibers as an alternative to cotton for textile applications. *International Journal of Biological Macromolecules*, *278*, 134630. https://doi.org/10.1016/j.ijbiomac.2024.134630

Nelson, D.L. and Cox, M.M. (2009). *Lehninger Principles of Biochemistry* (5th edn). W.H. Freeman and Company. New York, USA.

Obadi, M., Sun, J. and Xu, B. (2021). Highland barley: Chemical composition, bioactive compounds, health effects, and applications. *Food Research International*, *140*, 110065. https://doi.org/10.1016/j.foodres.2020.110065

Panajotova, H., Strinska, H., Gandova, V., Dobreva, V., Zhekova, B. and Dobrev, G. (2017). Purification of lipase from *Aspergillus carbonarius* NRRL369 by ATPS PEG/potassium phosphate. *Bulgarian Chemical Communications*, *49*, 130–136.

Phetlum, S. and Champasri, C. (2023). Purification and characterization of amylases from three freshwater fish species providing new insight application as enzyme molecular markers for zymography. *Fish Physiology and Biochemistry*, *49*(6), 1257–1276. https://doi.org/10.1007/s10695-023-01255-9

Pismag, R., Pico, J., Fernández, A., Hoyos, J. L. and Martinez, M.M. (2023). α-amylase reactive extrusion enhances the protein digestibility of saponin-free quinoa flour while preserving its total phenolic content. *Innovative Food Science & Emerging Technologies*, *88*, 103448. https://doi.org/10.1016/j.ifset.2023.103448

Polachini, T.C., Cárcel, J.A., Norwood, E.A., Chevallier, S.S., Le-Bail, P. and Le-Bail, A.

(2023). Hot-air ultrasound-assisted drying of green wheat and barley malts to enhance process kinetics, amylase activity and their application in bread formulation. *Food and Bioproducts Processing*, *142*, 17–28. https://doi.org/10.1016/j.fbp.2023.08.009

Posoongnoen, S., Thummavongsa, T., Junthip, J., Jandaruang, J. and Preecharram, S. (2025). Potential application of α-amylase from germinating *Cucurbita moschata* duchesne seeds in eco-friendly bioethanol production. *Scientific Reports*, *15*(1), 25499. https://doi.org/10.1038/s41598-025-11653-z

Rani, H., Standish, A., Walling, J.G. and Whitcomb, S.J. (2025). Development and quality assessment of low-cost benchtop malting protocol for laboratory-scale barley (Hordeum vulgare L.) malt quality evaluation. *Journal of Cereal Science*, *123*, 104138. https://doi.org/10.1016/j.jcs.2025.104138

Rao, K.H. and Haseena, S. (2024). Principles of basic and advanced techniques used for the purification of enzymes of industrial importance. In *Recent Advances in Bioprocess Engineering and Bioreactor Design,* (S. Dhagat, S.E. Jujjavarapu, N.S.S. Kumar and C. Mahapatra, eds.), Pp. 171-183. Springer Nature, Singapore.

Robles-Arias, M.A., Escalona-Buendía, H.B., Ramírez-Romero, M.A.G. and Cruz-Guerrero, A.E. (2025). Obtention of amaranth resistant starch through succinylation and phosphorylation reaction. *Revista Mexicana de Ingeniería Química*, *24*(2), 1–20. https://doi.org/10.24275/rmiq/Alim25547

Rodríguez-Herrera, V.V., García-Cruz, L. and Valle-Guadarrama, S. (2023). Aqueous two-phase extraction: A non-thermal technique to separate and concentrate betalains from *Bougainvillea glabra* Choisy bracts. *Industrial Crops and Products*, *193*, 116245. https://doi.org/10.1016/j.indcrop.2023.116245

Rodríguez-Salazar, N. and Valle-Guadarrama, S. (2020). Separation of phenolic compounds from roselle (*Hibiscus sabdariffa*) calyces with aqueous two-phase extraction based on sodium citrate and polyethylene glycol or acetone. *Separation Science and Technology*, *55*(13), 2313–2324. https://doi.org/10.1080/01496395.2019.1634730

Roth, C., Moroz, O.V., Turkenburg, J.P., Blagova, E., Waterman, J., Ariza, A., Ming, L., Tianqi, S. andersen, C., Davies, G.J. and Wilson, K.S. (2019). Structural and functional characterization of three novel fungal amylases with enhanced stability and pH tolerance. *International Journal of Molecular Sciences*, *20*(19), 4902. https://doi.org/10.3390/ijms20194902

Šalić, A., Ljubić, A., Marčinko, T., Jurinjak TuŠek, A., Cvjetko Bubalo, M., TiŠma, M. and Zelić, B. (2023). Shifting the natural deep eutectic solvent based liquid lipase extraction from batch to continuous for more efficient process performance. *Journal of Cleaner Production*, *405*, 136899. https://doi.org/10.1016/j.jclepro.2023.136899

Segel, I.H. (1993). *Enzyme kinetics: behavior and analysis of rapid equilibrium and steady-state enzyme systems*. Wiley-Interscience, USA.

Shad, Z., Mirhosseini, H., Hussin, A.S.M., Forghani, B., Motshakeri, M. and Manap, M. Y.A. (2018). Aqueous two-phase purification of α-Amylase from white pitaya (*Hylocereus undatus*) peel in polyethylene glycol /citrate system: Optimization by response surface methodology. *Biocatalysis and Agricultural Biotechnology*, *14*, 305–313. https://doi.org/10.1016/j.bcab.2018.01.014

Shirodkar, P.V., Muraleedharan, U.D., Damare, S. and Raghukumar, S. (2020). A mesohaline thraustochytrid produces extremely halophilic alpha-amylases. *Marine Biotechnology*, *22*(3), 403–410. https://doi.org/10.1007/s10126-020-09960-9

Singla, M. and Sit, N. (2023). Isolation of papain from ripe papaya peel using aqueous two-phase extraction. *Journal of Food Measurement and Characterization*, *17*(2), 1685–1692. https://doi.org/10.1007/s11694-022-01741-3

Sofi, S.A., Rafiq, S., Singh, J., Mir, S.A., Sharma, S., Bakshi, P., McClements, D.J., Mousavi Khaneghah, A. and Dar, B.N. (2023). Impact of germination on structural, physicochemical, techno-functional, and digestion properties of desi chickpea (Cicer arietinum L.) flour. *Food Chemistry*, *405*, 135011. https://doi.org/10.1016/j.foodchem.2022.135011

SPSS, I. (2000). *Sigma Plot 2000 User's Guide*. SPSS Inc., Chicago, IL, USA.

Sudeep, K.C., Upadhyaya, J., Joshi, D.R., Lekhak, B., Kumar Chaudhary, D., Raj Pant, B., Raj Bajgai, T., Dhital, R., Khanal, S., Koirala, N. and Raghavan, V. (2020). Production,

characterization, and industrial application of pectinase enzyme isolated from fungal strains. *Fermentation*, *6*(2), 59. https://doi.org/10.3390/fermentation6020059

The Mathworks Inc. (2008). *Optimization Toolbox™ 4 User's Guide*. The MathWorks, Inc., Natick, MA, USA.

Uno-Okamura, K., Soga, K., Wakabayashi, K., Kamisaka, S. and Hoson, T. (2004). Purification and properties of apoplastic amylase from oat (*Avena sativa*) seedlings. *Physiologia Plantarum*, *121*(1), 117–123. https://doi.org/10.1111/j.0031-9317.2004.00298.x

Van de Velde, F., Méndez-Galarraga, M.P., Albarracín, M., Garzón, A.G., Aquino, M., Cian, R.E., Vinderola, G. and Drago, S.R. (2025). Exploring the effects of barley (*Hordeum vulgare* L.) germination on chemical composition, phytic acid, and potential malt prebiotic properties. *Journal of Food Composition and Analysis*, *138*, 107016. https://doi.org/10.1016/j.jfca.2024.107016

Verlaine, O., Malempré, R., Versées, W., Matagne, A. and Frère, J.M. (2024). Single time-point analysis of product and substrate inhibition. *Scientific Reports*, *14*(1), 23160. https://doi.org/10.1038/s41598-024-70805-9

Wang, Y., Ral, J.P., Saulnier, L. and Kansou, K. (2022). How does starch structure impact amylolysis? Review of current strategies for starch digestibility study. *Foods*, *11*(9), 1223. https://doi.org/10.3390/foods11091223

Xie, C., Liu, Y., Su, L., Zhang, C., Li, D., Wang, P., Liu, J. and Yang, R. (2025). The effects of germination and different milling degrees on the nutritional properties of rice bran. *Journal of Cereal Science*, *124*, 104231. https://doi.org/10.1016/j.jcs.2025.104231

Yang, B., Yin, Y., Liu, C., Zhao, Z. and Guo, M. (2021). Effect of germination time on the compositional, functional and antioxidant properties of whole wheat malt and its end-use evaluation in cookie-making. *Food Chemistry*, *349*, 129125. https://doi.org/10.1016/j.foodchem.2021.129125

Zheng, J., Wang, N., Yang, J., You, Y., Zhang, F., Kan, J. and Wu, L. (2024). New insights into the interaction between bamboo shoot polysaccharides and lotus root starch during gelatinization, retrogradation, and digestion of starch. *International Journal of Biological Macromolecules*, *254*, 127877. https://doi.org/10.1016/j.ijbiomac.2023.127877

Zhu, H., Bai, X., Liang, Q., Zhong, L., Chang, H., Chen, Y. and Qiao, Z. (2024). Study on multi-stage aqueous two-phase extraction of papain. *Food and Fermentation Industries*, *50*(4), 152–156. https://doi.org/10.13995/j.cnki.11-1802/ts.035787